

## THE EQUATORIAL BACKGROUND SOLAR CORONA DURING SOLAR MINIMUM

R. RAMESH,<sup>1</sup> H. S. NATARAJ,<sup>2</sup> C. KATHIRAVAN,<sup>2</sup> AND CH. V. SASTRY<sup>3</sup>

Received 2005 April 15; accepted 2006 May 9

### ABSTRACT

We report two-frequency (51 and 77 MHz) radio observations of the equatorial brightness distribution of the “undisturbed” solar corona, close to the minimum between sunspot cycles 22 and 23. The contributions from different discrete structures in the observed one-dimensional profiles were identified and removed through an iterative multi-Gaussian least-squares curve fitting technique, and the “background” corona was obtained for each observation. Its average east-west (E-W) diameter is  $43' \pm 4'$  and  $38' \pm 2'$  at 51 and 77 MHz respectively. This indicates that the plasma levels corresponding to the above two frequencies are located at radial distances ( $r$ , measured from center of the Sun) of  $\approx 1.35$  and  $1.19 R_{\odot}$ ; and the electron density ( $N_e$ ) there is  $3.2$  and  $7.3 \times 10^7 \text{ cm}^{-3}$ , respectively. Using the above values, we derived the corresponding density gradient,  $\propto r^{-6.5}$ . We also calculated the integrated flux densities ( $S$ ) of emission from the background corona; the average values are  $\approx 0.46$  and  $1.12 \text{ sfu}$  ( $1 \text{ sfu} = \text{solar flux unit} = 10^{-22} \text{ W m}^{-2} \text{ Hz}^{-1}$ ) at the above two frequencies. The corresponding brightness temperatures ( $T_b$ ) are  $3.85$  and  $5.44 \times 10^5 \text{ K}$ . We estimated the spectral dependence of the former, finding that it scales as  $\nu^{2.2}$ , where  $\nu$  is the frequency of observation. The day-to-day values of the E-W diameter show significant variation at both 51 and 77 MHz, even after the removal of contributions from discrete sources.

*Subject headings:* scattering — Sun: activity — Sun: corona — Sun: radio radiation

### 1. INTRODUCTION

The density structure of the large-scale corona is traditionally probed using white-light (polarized brightness) data via a van de Hulst (1950a, 1950b) inversion. This method assumes that the polarized brightness of white light is caused by Thomson scattering and is proportional to the line-of-sight integrated coronal electron density. Some of the density models that are frequently used at present were deduced in this fashion through observations during total solar eclipse (Baumbach 1937; Allen 1947; Saito 1970) with coronagraphs atop high-altitude mountain ranges (Newkirk 1961) and on board space missions (Saito et al. 1977). Each eclipse provides at most only a few hours of observation, and it is not possible to assess the contribution of streamers to the measured coronal radiation. This raises the question as to whether or not any given measurement accurately represents only the “background” corona (Saito et al. 1977). For observations with a coronagraph, its occulting disk covers both the solar disk and its atmosphere up to a certain height, so it cannot observe the corona overlying the solar disk, as well as that beyond the limb, until a certain distance. The radial variations of electron density have also been obtained using direct in situ observations (Bougeret et al. 1984), the frequency drift rate of type III radio bursts (Leblanc et al. 1998 and references therein), and numerical solutions of the magnetohydrostatic equation (Mann et al. 1999). However, they apply mostly to the outer corona and interplanetary space. There have also been estimates through density-sensitive spectral lines (Fludra et al. 1999; Gallagher et al. 1999) and soft X-ray data (Aschwanden & Acton 2001) in the off-limb region.

Measurements of radio emission from the background solar corona (i.e., the corona distinct from emission due to rapidly and slowly varying discrete sources associated with flares, active regions, streamers, filaments, arches, holes, etc.) are useful in

deriving physical properties such as electron density or temperature that characterize different layers of the solar atmosphere. Observations can be made from the ground, regardless of atmospheric conditions. Again, the corona overlying the visible solar disk can be observed. In addition, the simplicity of the emission process (Martyn 1946; Ginzburg 1946) and radiative transfer (Smerd 1950) make radio techniques an attractive and useful tool to investigate the characteristics of the “undisturbed” Sun.

Observations at frequencies  $< 100 \text{ MHz}$  play a useful role in this connection, since the radiation originates fully in the corona. Such work has been carried out by several authors in the past (O’Brien 1953; Sheridan 1970; Aubier et al. 1971; Erickson et al. 1977; Kundu et al. 1977; Gergely et al. 1985; Subramanian & Sastry 1988; Thejappa & Kundu 1992; Sastry 1994; Ramesh 2000; Subramanian 2004). But the observed radio brightness distribution shows several kinds of localized structures even in the absence of solar activity: bright regions that are usually related to coronal streamers, intermediate “quiet” regions that correspond to moderately bright looplike structures seen in soft X-rays, and dark regions corresponding to coronal holes (Sheridan & Dulk 1980). Historically, the minimum envelope in the superposition of an east-west (E-W) one-dimensional brightness distribution obtained every day for a considerable period of time is taken as representative of the background corona at radio frequencies, and its half-power width is assumed to be the solar diameter at the corresponding observing frequency (Pawsey & Yabsley 1949; Leblanc & Le Squeren 1969). The ideal method for identifying the background corona is to use an antenna system with high angular resolution so that the aforementioned structures can be clearly distinguished. But existing large arrays such as the Very Large Array and the Giant Metrewave Radio Telescope operate mainly at higher frequencies. They also do not have sufficient ( $u, v$ ) coverage at low spatial frequencies to image the background corona and the large-scale structures there (Mercier et al. 2006).

### 2. OBSERVATIONS

The data reported were obtained in 1995 February with the E-W arm of the Gauribidanur radioheliograph (GRH; Ramesh

<sup>1</sup> Centre for Research and Education in Science and Technology, Indian Institute of Astrophysics, Hosakote 562 114, India; ramesh@iiap.res.in.

<sup>2</sup> Indian Institute of Astrophysics, Bangalore 560 034, India; nataraj@iiap.res.in, kathir@iiap.res.in.

<sup>3</sup> MEENAKSHI, Number 3, 2nd Cross, 1st Block, Koramangala, Bangalore 560 034, India; claxmi64@hotmail.com.

et al. 1998) operating near Bangalore in India. The southern arm of the array was under construction at that time, so, we have only E-W one-dimensional data. We specifically selected the above data set, since the epoch of observation was close to the minimum between sunspot cycles 22 and 23, and we also had simultaneous observations at two frequencies. The active regions on the Sun are located mostly close to the equatorial plane during the sunspot minimum period. Again, there are usually fewer than at the solar maximum. Hence, the use of a one-dimensional data set is an advantage for the present work, since structures at different heliographic longitude can be identified with a factor of 2 better angular resolution compared to observations using a two-dimensional array of antennas (Christiansen & Högbom 1985, p. 126). The minimum detectable flux limit of the array is  $\approx 0.02$  sfu, and the angular resolution is  $7'$  and  $4'$  at 51 and 77 MHz, respectively. The integration time used was 256 ms. The calibration scheme for GRH data makes use of redundancy in the length and orientation of various baseline vectors in the array and enables us to image the solar corona with a dynamic range of  $\geq 20$  dB (Ramesh 1998, p. 57; Ramesh et al. 1999a; Kathiravan 2005, p. 18). This is useful in detecting thermal emission associated with weak density enhancements in the solar atmosphere in a better manner.

The array gain was estimated using observations of the sidereal source Hydra A, located in the same declination range as the Sun during the observing period reported. The calibrated outputs from different baselines were Fourier transformed to synthesize the E-W one-dimensional brightness distribution. The sidelobe contributions were removed using the CLEAN algorithm (Högbom 1974). We selected only those observations during which the solar corona was undisturbed and no X-ray/ $H\alpha$  flares or nonthermal radio burst activity were reported (Solar-Geophysical Data, 1995 April, August). We also checked for the existence of large polar coronal holes in our observing period, which otherwise might affect the measurements since they are usually extended in the same direction (north-south [N-S]) as the fan beam of an E-W array (Lantos 1980), but there were none. Again, only data obtained close to the local noon at Gauribidanur ( $\approx 06:30$  UT) were considered, since refraction effects due to Earth's ionosphere are expected to be minimal around that time (Stewart & McLean 1982).

### 3. THE METHOD

To start with we assumed that (1) the density and temperature structure of different localized sources in our observations follow a Gaussian distribution and (2) the visibility of a particular source depends on its size, strength, and relative location from the disk center. It may appear either prominently or just as a change in the slope of the observed distribution at the corresponding position. For example, the contrast of a source corotating with the Sun will be higher when it is close to/off the limb, since the optical depth of the background corona will be relatively smaller there (Lantos et al. 1987; Alissandrakis 1994). On this basis, we adopted the following steps/criteria to determine the background corona in the present case:

1. Each observed brightness distribution was reproduced using an iterative multi-Gaussian least-squares curve fitting technique.
2. The amplitude at any location in the distribution is the sum of the amplitude of different Gaussian profiles used for the fit at that location.
3. The minimum width of the Gaussian profile was limited to 2.5, the smallest source size ever observed at frequencies  $< 100$  MHz (Ramesh et al. 1999b; Ramesh & Sastry 2000).

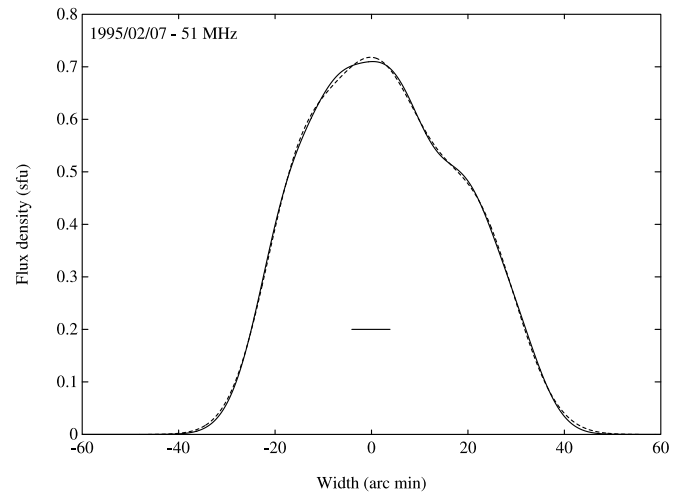


FIG. 1.—Equatorial brightness distribution of the solar corona obtained with the E-W arm of the GRH at 51 MHz on 1995 February 7, around local noon ( $\approx 06:30$  UT). The profiles shown in solid and dashed lines are the observed brightness distribution and its least-squares fit, respectively. The horizontal line close to the center indicates the angular resolution of the array in the E-W direction.

4. The maximum number of Gaussian profiles was restricted to 20, since the half-power diameter of the undisturbed solar corona is not expected to be  $> 3 R_{\odot}$  in our frequency range, even under the extreme case of scattering by density inhomogeneities (McMullin & Helfer 1977; Thejappa & Kundu 1992).

5. The discrete sources identified from the fit should be present at both 51 and 77 MHz on any given day.

6. Only those observations for which the fit consists of a Gaussian profile with angular width  $> 32'$  (the angular size of the solar photosphere) were considered for further study.

7. The peak of the Gaussian profile whose width is  $> 32'$  should be located close to the transit time of the Sun over the local meridian at Gauribidanur ( $\approx 06:30$  UT). Ionospheric refraction effects, if any, are taken care of by this condition.

Figures 1 and 2 show the observed equatorial brightness distribution of the solar corona (*solid line*) and its least-squares fit (*dashed line*) on 1995 February 7 at 51 and 77 MHz, respectively. There is a good correspondence between the observations and their fits at both frequencies. The different Gaussian profiles corresponding to the aforementioned least-squares fit are shown in Figures 3 and 4. The number of Gaussian profiles and their respective locations are same at both frequencies. Figures 5 and 6 show the interday changes in the E-W diameter after the removal of the contributions from discrete sources. The variations are more pronounced at 51 MHz than at 77 MHz.

### 4. ANALYSIS AND RESULTS

Considering the Gaussian profile in criterion 7 of § 3 as the best representative of the background corona, we estimated its integrated flux density and half-power width from the fit for each observation. The respective average values at 51 MHz are  $0.46 \pm 0.02$  sfu and  $43' \pm 4'$ . The corresponding values at 77 MHz are  $1.12 \pm 0.02$  sfu and  $38' \pm 2'$ . We calculated the flux density spectral index of the observed emission using the aforementioned data, and obtained  $\approx 2.2 \pm 0.2$ . This indicates that it is mostly thermal. Note that Erickson et al. (1977) previously reported observations of the undisturbed Sun in the same frequency range during 1976 July–August, and the estimated index was  $\approx 2.3$ . The authors had assumed the solar brightness distribution to be a disk of uniform brightness temperature for

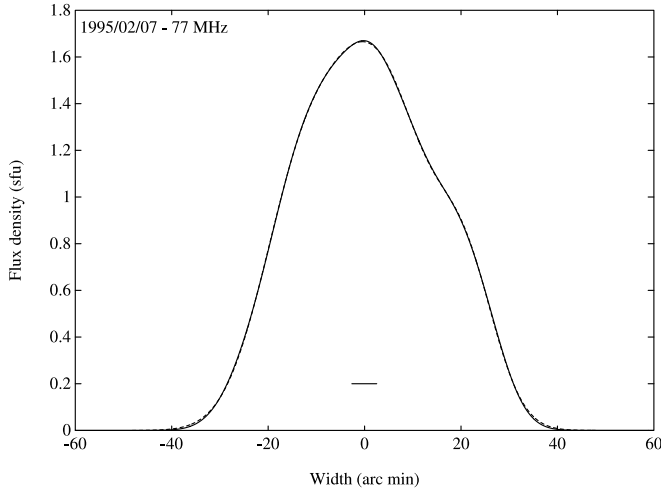


FIG. 2.—Same as Fig. 1, but at 77 MHz. There is a close correspondence between the observation and its fit in both cases.

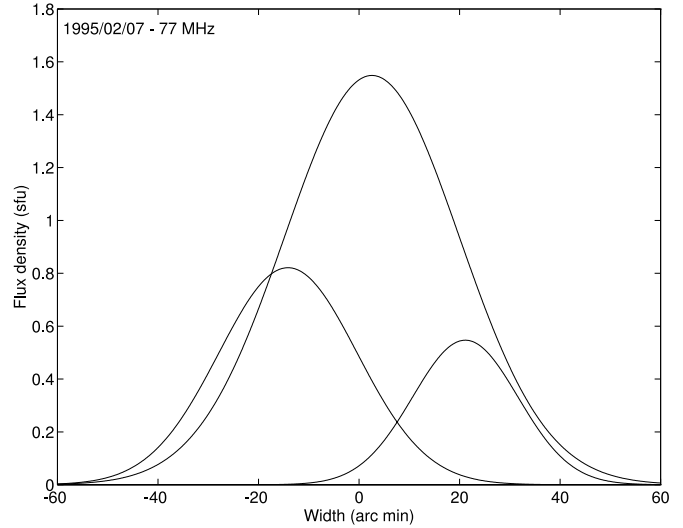


FIG. 4.—Same as Fig. 3, but for the fit in Fig. 2. The number of Gaussian profiles and their respective locations are the same as in Fig. 3.

their calculations. A similar study was carried out by Subramanian & Sastry (1988) during 1985 May–September, but their result shows a large variation in the range 1.6–3.9, unlike the previous work.

Assuming the N-S diameter of the solar corona during solar minimum to be approximately 0.82 times the E-W diameter in our frequency range (Gergely et al. 1985; Thejappa & Kundu 1992), we calculated the brightness temperature of the background corona, obtaining  $3.85$  and  $5.44 \times 10^5$  K at 51 and 77 MHz, respectively. This is about an order of magnitude higher than the lowest  $T_b$  ever reported for the “radio” Sun in the same frequency range (Thejappa & Kundu 1992).

The major contribution to the optical depth of the radio radiation at any particular frequency comes mainly from a small spherical shell above the layer where the plasma frequency in the solar atmosphere equals the observing frequency. Therefore, the distance of the shell from center of the Sun can be considered as the radial distance from which the observed emission originates. As mentioned earlier, the average half-power diameters

of the observed brightness distribution in the present case are  $43' \pm 4'$  and  $38' \pm 2'$  at 51 and 77 MHz, respectively. Based on this, we calculated the radial distance of the plasma level corresponding to the above two frequencies, obtaining  $\approx 1.35$  and  $1.19 R_\odot$ , respectively.

The plasma densities corresponding to 51 and 77 MHz are  $3.2 \times 10^7$  and  $7.3 \times 10^7 \text{ cm}^{-3}$ , respectively. In the present case, these are the electron density values at  $\approx 1.35$  and  $1.19 R_\odot$  from center of the Sun. Assuming that  $N_e \propto r^\beta$ , we have

$$(N_e)_{51} \propto 1.35^\beta, \tag{1}$$

$$(N_e)_{77} \propto 1.19^\beta, \tag{2}$$

i.e.,

$$\frac{(N_e)_{51}}{(N_e)_{77}} = \left(\frac{1.35}{1.19}\right)^\beta. \tag{3}$$

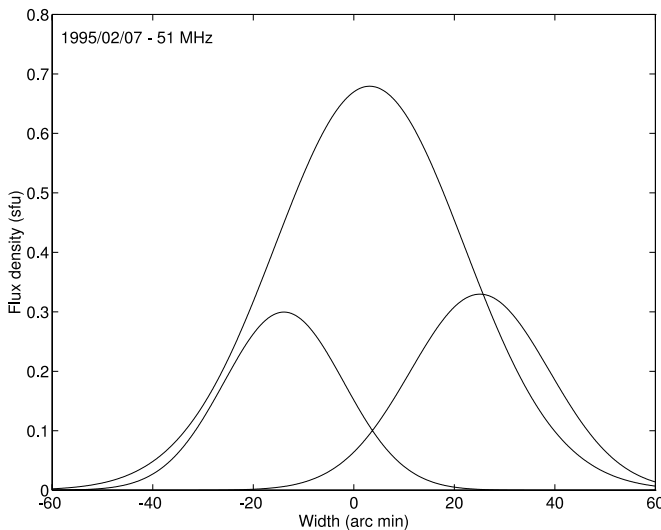


FIG. 3.—Different Gaussian distributions corresponding to the fit in Fig. 1. The profile with the largest amplitude and broadest width corresponds to the “background.” The other two on either side of the center and with relatively smaller amplitudes correspond to discrete sources.

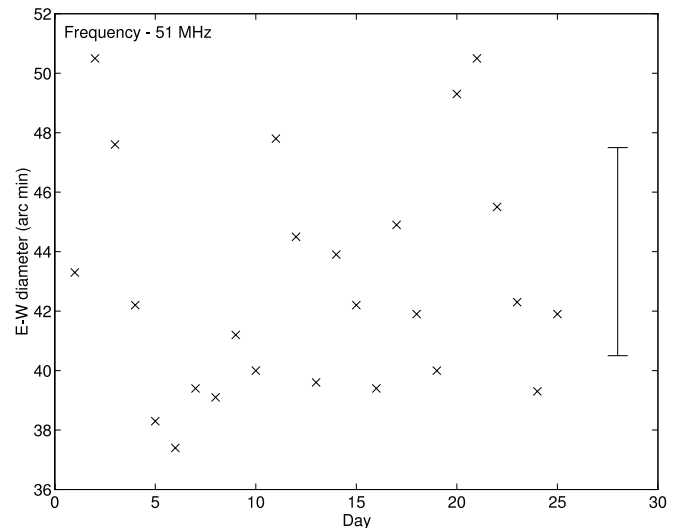


FIG. 5.—Day-to-day variation in the E-W diameter of the “background” solar corona at 51 MHz after the removal of contribution from discrete sources. The vertical line on the right side shows the error in each measurement.

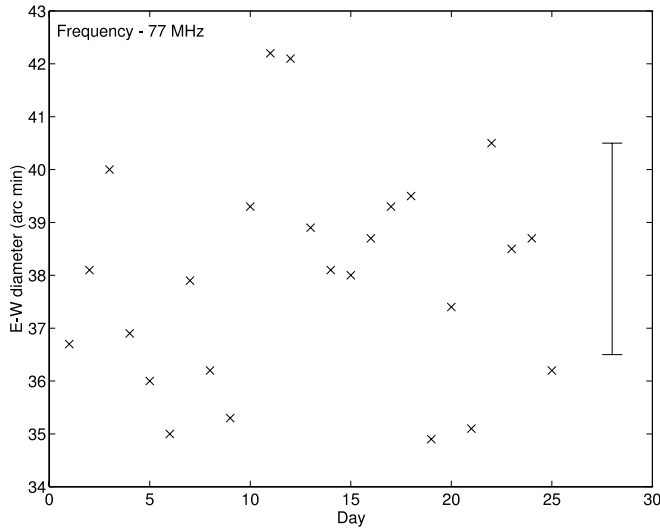


FIG. 6.—Same as Fig. 5, but at 77 MHz.

On substituting the corresponding values for  $(N_e)_{51}$  and  $(N_e)_{77}$  and using the logarithm on both sides of equation (3), we get  $\beta = -6.5$ . This implies that the variation in the electron density distribution of the background corona  $\propto r^{-6.5}$ , in the above radial distance range. Note that only Saito et al. (1977) had reported the electron density of the background corona alone prior to the present work. Using data obtained with the white-light coronagraph on board *SkyLab*, they found that the density varies as  $r^{-6}$  in the distance range  $2.5$ – $5.5 R_\odot$ . Our result is consistent with theirs. However, the earlier estimate of the radio Sun diameter in about the same frequency range as the present case indicates that the density variation  $\propto r^{-4.4}$  (Aubier et al. 1971; Gergely et al. 1985). It is possible that this index represents a “global” variation including contributions from discrete sources. To verify this, we calculated the density variation using E-W diameter values at 73.8, 50, and 38.5 MHz reported by Thejappa & Kundu (1994), who found well-identified streamers near the east and west limbs in the corresponding white-light data. The result was  $r^{-3.4}$ . Again Ramesh et al. (2000) noted that the density associated with the discrete radio source observed by them at 51 and 77 MHz varies as  $r^{-1.8}$ . These results strengthen the above argument.

Doyle et al. (1999) estimated the density associated with long-lived large-scale structures such as coronal holes in the distance range  $\sim 1$ – $2 R_\odot$  using *Solar and Heliospheric Observatory (SOHO)* SUMER data, and the variation  $\propto r^{-8}$ . Similar work was carried out for streamers through *SOHO* UVCS and *Yohkoh* SXT observations by Li et al. (1998) and *SOHO* LASCO and Mauna Loa K-coronagraph data by Gibson et al. (1999). They found that the density varies as  $r^{-8.6}$ . The density gradient associated

with a particular discrete structure also depends on whether it is new or old; nevertheless, it is always different from that of the background corona (Leblanc et al. 1970).

An inspection of Figures 5 and 6 indicates that there is noticeable variation in the day-to-day values of the E-W diameter at both 51 and 77 MHz, even after the removal of contributions from discrete sources. The half-power diameter of the background equatorial corona varies from  $36'$  to  $52'$  and  $34'$  to  $43'$  at the above two frequencies, respectively. One possible reason for this could be irregular refraction effects due to density fluctuations in the corona that vary as  $\nu^{-2}$  (Fokker 1965; Aubier et al. 1971; Steinberg et al. 1971; Caroubalos et al. 1972; Riddle 1974; Bougeret & Steinberg 1977; Duncan 1979; Robinson 1983; Thejappa & Kundu 1992; Bastian 1994; Ramesh et al. 2001). The magnitude of variation being greater at 51 MHz than at 77 MHz probably indicates the same. However, this needs to be verified quantitatively through ray-tracing calculations or by solving the radiative transfer equation, including scattering.

## 5. CONCLUSIONS

We studied the characteristics of radio emission from the equatorial “background” solar corona during 1995 February (close to the minimum between sunspot cycles 22 and 23) at 51 and 77 MHz, after eliminating the contributions of various discrete sources to the observed E-W one-dimensional brightness distribution through an iterative multi-Gaussian least-squares curve-fitting technique. Our results are:

1. The average E-W diameter and integrated flux density are  $43'$  and  $38'$  and  $0.46$  and  $1.12$  sfu, respectively, at the above two frequencies. The corresponding brightness temperatures are  $3.85$  and  $5.44 \times 10^5$  K.
2. The plasma levels corresponding to 51 and 77 MHz radio radiation are located at radial distances of  $\approx 1.35$  and  $1.19 R_\odot$ , from the center of the Sun.
3. The electron density distribution varies as  $r^{-6.5}$  in the above distance range.
4. The flux density spectral index ( $\alpha$ ) of radio emission in the frequency range 51–77 MHz is  $\approx 2.2$ .
5. There is considerable variation in the day-to-day value of the E-W diameter even after the removal of contributions from discrete sources.

We thank the staff of the Gauribidnaur radio observatory for their help in maintaining the antenna and receiver systems there. We particularly acknowledge C. N. Gowda, A. A. Saheb, and G. N. Rajasekara for their assistance in obtaining data with GRH. We are grateful to the referee for his/her remarks, which motivated us to rewrite and clearly bring out the results.

## REFERENCES

- Alissandrakis, C. E. 1994, *Adv. Space Res.*, 14(4), 81  
 Allen, C. W. 1947, *MNRAS*, 107, 426  
 Aschwanden, M. J., & Acton, L. W. 2001, *ApJ*, 550, 475  
 Aubier, M., Leblanc, Y., & Boischoat, A. 1971, *A&A*, 12, 435  
 Bastian, T. S. 1994, *ApJ*, 426, 774  
 Baumbach, S. 1937, *Astron. Nachr.*, 263, 120  
 Bougeret, J.-L., King, J. H., & Schwenn, R. 1984, *Sol. Phys.*, 90, 401  
 Bougeret, J.-L., & Steinberg, J.-L. 1977, *A&A*, 61, 777  
 Caroubalos, C., et al. 1972, *A&A*, 16, 374  
 Christiansen, W. N., & Högbom, J. A. 1985, *Radio Telescopes* (Cambridge: Cambridge Univ. Press)  
 Doyle, J. G., Teriaca, L., & Banerjee, D. 1999, *A&A*, 349, 956  
 Duncan, R. A. 1979, *Sol. Phys.*, 63, 389  
 Erickson, W. C., et al. 1977, *Sol. Phys.*, 54, 57  
 Fludra, A., et al. 1999, *J. Geophys. Res.*, 104, 9709  
 Fokker, A. D. 1965, *Bull. Astron. Inst. Netherlands*, 18, 111  
 Gallagher, P. T., et al. 1999, *ApJ*, 524, L133  
 Gergely, T. E., Gross, B. D., & Kundu, M. R. 1985, *Sol. Phys.*, 99, 323  
 Gibson, S. E., et al. 1999, *J. Geophys. Res.*, 104, 9691  
 Ginzburg, V. L. 1946, *CR Acad. Sci. URSS*, 52, 487  
 Högbom, J. A. 1974, *A&AS*, 15, 417  
 Kathiravan, C. 2005, Ph.D. thesis, Mangalore Univ.  
 Kundu, M. R., Gergely, T. E., & Erickson, W. C. 1977, *Sol. Phys.*, 53, 489  
 Lantos, P. 1980, in *IAU Symp. 86, Radio Physics of the Sun*, ed. M. R. Kundu & T. E. Gergely (Dordrecht: Reidel), 41  
 Lantos, P., et al. 1987, *Sol. Phys.*, 112, 325

- Leblanc, Y., Dulk, G. A., & Bougeret, J.-L. 1998, *Sol. Phys.*, 183, 165  
Leblanc, Y., Leroy, J. L., & Poulain, P. 1970, *A&A*, 5, 391  
Leblanc, Y., & Le Squeren, A. M. 1969, *A&A*, 1, 239  
Li, J., et al. 1998, *ApJ*, 506, 431  
Mann, G., et al. 1999, *A&A*, 348, 614  
Martyn, D. F. 1946, *Nature*, 158, 632  
McMullin, J. N., & Helfer, H. L. 1977, *Sol. Phys.*, 53, 471  
Mercier, C., et al. 2006, *A&A*, 447, 1189  
Newkirk, G., Jr. 1961, *ApJ*, 133, 983  
O'Brien, P. A. 1953, *MNRAS*, 113, 597  
Pawsey, J. L., & Yabsley, D. E. 1949, *Australian J. Sci. Res. A*, 2, 198  
———. 2000, *J. Astrophys. Astron.*, 21, 237  
Ramesh, R., Kathiravan, C., & Sastry, Ch. V. 2001, *ApJ*, 548, L229  
Ramesh, R., & Sastry, Ch. V. 2000, *A&A*, 358, 749  
Ramesh, R., Subramanian, K. R., & Sastry, Ch. V. 1999a, *A&AS*, 139, 179  
———. 1999b, *Sol. Phys.*, 185, 77  
———. 2000, *Astron. Lett. Commun.*, 40, 93  
Ramesh, R., et al. 1998, *Sol. Phys.*, 181, 439  
Riddle, A. C. 1974, *Sol. Phys.*, 35, 153  
Robinson, R. D. 1983, *Proc. Astron. Soc. Australia*, 5(2), 208  
Saito, K. 1970, *Ann. Tokyo Astron. Obs.*, Ser. 2, 12, 53  
Saito, K., Poland, A. I., & Munro, R. H. 1977, *Sol. Phys.*, 55, 121  
Sastry, Ch. V. 1994, *Sol. Phys.*, 150, 285  
Sheridan, K. V. 1970, *Proc. Astron. Soc. Australia*, 1(7), 304  
Sheridan, K. V., & Dulk, G. A. 1980, in *IAU Symp. 91, Solar and Interplanetary Dynamics*, ed. M. Dryer & E. Tandberg-Hanssen (Dordrecht: Reidel), 37  
Smerd, S. F. 1950, *Australian J. Sci. Res. A*, 3, 34  
Steinberg, J. L., et al. 1971, *A&A*, 10, 362  
Stewart, R. T., & McLean, D. J. 1982, *Proc. Astron. Soc. Australia*, 4(4), 386  
Subramanian, K. R. 2004, *A&A*, 426, 329  
Subramanian, K. R., & Sastry, Ch. V. 1988, *J. Astrophys. Astron.*, 9, 225  
Thejappa, G., & Kundu, M. R. 1992, *Sol. Phys.*, 140, 19  
———. 1994, *Sol. Phys.*, 149, 31  
van de Hulst, H. C. 1950a, *Bull. Astron. Inst. Netherlands*, 11, 135  
———. 1950b, *Bull. Astron. Inst. Netherlands*, 11, 150